JOC Article

Magnesium Ion Selective Two-Photon Fluorescent Probe Based on a Benzo[*h*]chromene Derivative for in Vivo Imaging

Hwan Myung Kim,† Pil Rye Yang,† Mun Sik Seo,† Jae-Sung Yi,‡ Jin Hee Hong,§ Seung-Joon Jeon,† Young-Gyu Ko,‡ Kyoung J. Lee,§ and Bong Rae Cho*,†

Molecular Opto-Electronics Laboratory, Department of Chemistry and Center for Electro- and Photo-Responsive Molecules, Graduate School of Life Sciences and Biotechnology, National Creative Research Initiative Center for Neurodynamics and Department of Physics, Korea University, 1-Anamdong, Seoul 136-701, Korea

chobr@korea.ac.kr

Received November 14, 2006

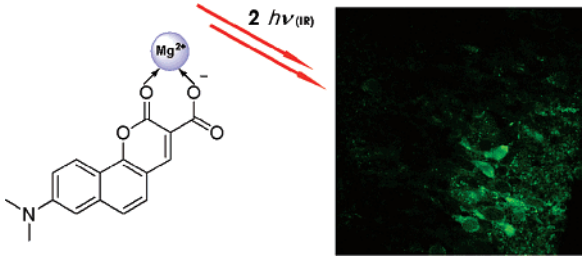

A novel, two-photon probe for the detection of free Mg^{2+} ions in living cells and live tissues has been developed. The probe can be excited by 880 nm laser photons, emits strong two-photon excited fluorescence in response to Mg^{2+} ions, can be easily loaded into the cell and tissue, shows high photostability, and can measure the Mg^{2+} ion concentration without interference by Ca^{2+} ions in living cells. The intracellular dissociation constant (K_d^i) for Mg^{2+} determined by the two-photon process is 2.5 mM, which is suitable for dynamic Mg^{2+} concentration measurement. In addition, the probe is capable of imaging endogenous stores of free Mg^{2+} at a few hundred micrometers depth in live tissues using two-photon microscopy (TPM).

Introduction

Optical imaging with two-photon microscopy (TPM) has become a vital tool in the investigation of living systems. Whereas one-photon microscopy (OPM) uses one photon of higher energy for the excitation, TPM utilizes two photons of lower energy to obtain the excited-state fluorophores. The advantages of TPM over OPM are localized excitation, increased penetration depth (>500 μm), lower tissue autofluorescence and self-absorption, in addition to the reduced photodamage and photobleaching.[1,2] The extra penetration that TPM affords is of particular interest in the tissue imaging because surface preparation artifacts such as damaged cells extend >70 μm into the brain slice interior.[3] However, the progress in this field is hindered by the lack of efficient two-photon probes for specific applications. Although a few examples of TP probes specific for metal ions, fluoride, and pH have been reported, they have been studied in organic solvents or in model membranes and are not useful for biological imaging.[4,5] Moreover, most of the fluorescent probes presently used for TPM are Mag-fura-2, Magnesium Green (MgG), and Oregon Green 488 BATPA-1

* To whom correspondence should be addressed. Telephone: 82-2-3290-3129. Fax: 82-2-3290-3121.

† Molecular Opto-Electronics Laboratory, Department of Chemistry and Center for Electro- and Photo-Responsive Molecules.

‡ Graduate School of Life Sciences and Biotechnology.

§ National Creative Research Initiative Center for Neurodynamics and Department of Physics.

(1) (a) Denk, W.; Strickler, J. H.; Webb, W. W. *Science* **1990**, *248*, 73−76. (b) So, P. T. C.; Dong, C. Y.; Masters, B. R.; Berland, K. M. *Annu. Rev. Biomed. Eng.* **2000**, *2*, 399−429.

(2) (a) Cahalan, M. D.; Parker, I.; Wei, S. H.; Miller, M. J. *Nat. Rev. Immunol.* **2002**, *2*, 872−880. (b) Zipfel, W. R.; Williams, R. M.; Webb, W. W. *Nat. Biotechnol.* **2003**, *21*, 1369−1377. (c) Helmchen, F.; Denk, W. *Nat. Methods* **2005**, *2*, 932−940.

(3) Williams, R. M.; Zipfel, W. R.; Webb, W. W. *Curr. Opin. Chem. Biol.* **2001**, *5*, 603−608.

(4) (a) Pond, J. K. J.; Tsutsumi, O.; Rumi, M.; Kwon, O.; Zojer, E.; Brédas, J.-L.; Marder, S. R.; Perry, J. W. *J. Am. Chem. Soc.* **2004**, *126*, 9291−9306. (b) Kim, H. M.; Jeong, M.-Y.; Ahn, H. C.; Jeon, S.-J.; Cho, B. R. *J. Org. Chem.* **2004**, *69*, 5749−5751. (c) Ahn, H. C.; Yang, S. K.; Kim, H. M.; Li, S.; Jeon, S.-J.; Cho, B. R. *Chem. Phys. Lett.* **2005**, *410*, 312−315.

10.1021/jo062341m CCC: $37.00 © 2007 American Chemical Society
Published on Web 02/23/2007

(OG) based on fluoroscein or benzofuran as the fluorophore having small two-photon cross sections (δ_{TPA} < 50 GM),[6] and therefore, there is a pressing need for more efficient TP probes with larger two-photon cross sections for in vivo imaging.

The Mg^{2+} ion is one of the most abundant divalent ions in the cell and plays crucial roles in cell proliferation and cell death as well as participates in the modulation of signal transduction, various transporters, and ion channels.[7−12] To understand its role in regulating cellular processes, it is important to monitor the Mg^{2+} concentration in the intracellular compartment as well as its distribution throughout living systems. Of the methods to determine the Mg^{2+} levels in the cell, which include atomic absorbance,[13] Mg^{2+}-selective electrodes,[14,15] null-point titration techniques,[14,16,17] and NMR,[14,18] only the imaging method using fluorescent dyes reports the spatial-temporal patterns of Mg^{2+} mobilization. A number of fluorescent Mg^{2+} probes such as Mag-fura-2 and MgG have been developed,[6] but these probes suffer from a Ca^{2+} interference because of stronger binding affinity for Ca^{2+} than for Mg^{2+}. To overcome this problem, a series of Mg^{2+} probes having a β-diketone binding site and a coumarine and fluorescein fluorophore (KMGs) that show higher selectivity for Mg^{2+} than for Ca^{2+} have been reported.[19] Very recently, it was reported that diaza-18-crown-6 hydroxyquinoline derivatives (DCHQ) are useful for the selective detection of Mg^{2+} in mammary cells by using TPM.[20] However, there is no report on an efficient TP probe with a significant two-photon cross section that is capable of imaging Mg^{2+} ions in live tissues.

To design an efficient TP probe for intracellular free Mg^{2+} ions, we considered several requirements: (i) a significant two-photon cross section in the 800−1000 nm range necessary to obtain a clear TPM image at low dye concentration; (ii) high selectivity for Mg^{2+} ions; (iii) sufficient water solubility for staining; and (iv) high photostability. In this paper, we present the development and characterization of a TP probe highly selective for the intracellular free Mg^{2+} ions (Chart 1). We have introduced a strong donor−acceptor pair in the cyclic planar framework to facilitate the intramolecular charge transfer (ICT) for the high δ_{TPA},[21] conjugated double bonds within a cycle to enhance the photostability,[22] and an integral β-keto acid as the Mg^{2+} ion receptor to increase the water solubility, while maintaining a small MW for optimal cell permeability. The β-keto acid is adopted from the fluorescent probes named KMGs because it shows stronger affinity for Mg^{2+} than for Ca^{2+}.[19]

Herein, we report a useful TP probe, CMg1, that can be excited by 880 nm laser photons and can selectively detect intracellular Mg^{2+} ions in a living Hep3B cell and in live mouse tissue with no Ca^{2+} interference and little background emission due to the membrane-bound probes.

CHART 1. Structures of CMg1, CMg1−AM, and CMg1−Mg^{2+} Complexes

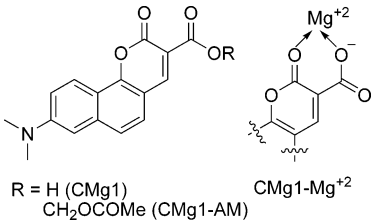

SCHEME 1. Synthetic Route for CMg1 and CMg1−AM[a]

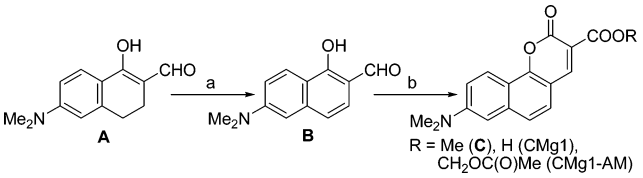

[a] Reagents and conditions: (a) DDQ/THF; (b) $CH_2(COOMe)_2$/piperidinium acetate/toluene.

Results and Discussion

CMg1 was synthesized in two steps starting from **A** (Scheme 1). Oxidation of **A** with DDQ afforded **B**, which was then subjected to the condensation with dimethyl malonate and hydrolysis to obtain CMg1. To improve the cell permeability, CMg1 was converted to acetoxymethyl (AM) ester (CMg1−AM).

Water solubility was determined by measuring the fluorescence intensity as a function of the dye concentration (Sup-

(5) (a) Werts, M. H. W.; Gmouh, S.; Mongin, O.; Pons, T.; Blanchard-Desce, M. *J. Am. Chem. Soc.* **2004**, *126*, 16294−16295. (b) Liu, Z.-Q.; Shi, M.; Li, F.-Y.; Fang, Q.; Chen, Z.-H.; Yi, T.; Huang, C.-H. *Org. Lett.* **2005**, *7*, 5481−5484.

(6) *The Handbooks−A Guide to Fluorescent Probes and Labeling Technologies*, 10th ed.; Haugland, R. P., Ed.; Molecular Probes: Eugene, OR, 2005.

(7) Hartwig, A. *Mutat. Res.* **2001**, *475*, 113−121.

(8) O'Rourke, B.; Backx, P. H.; Marban, E. *Science* **1992**, *257*, 245−248.

(9) Politi, H. C.; Preston, R. R. *Neuroreport* **2003**, *14*, 659−668.

(10) Dai, L.-J.; Ritchie, G.; Kerstan, D.; Kang, H. S.; Cole, D. E. C.; Quamme, G. A. *Physiol. Rev.* **2001**, *81*, 51−84.

(11) Schmitz, C.; Perraud, A.; Johnson, C. O.; Inabe, K.; Smith, M. K.; Penner, R.; Kurosaki, T.; Fleig, A.; Scharenberg, A. M. *Cell* **2003**, *113*, 191−200.

(12) Wolf, F. I.; Torsello, A.; Fasanella, A.; Cittadini, A. *Mol. Aspects Med.* **2003**, *24*, 11−25.

(13) (a) Wolf, F. I.; Di Francesco, A.; Cittadini, A. *Arch. Biochem. Biophys.* **1994**, *308*, 335−341. (b) Di Francesco, A.; Desnoyer, R. W.; Covacci, V.; Wolf, F. I.; Romani, A.; Cittadini, A.; Bond, M. *Arch. Biochem. Biophys.* **1998**, *360*, 149−157.

(14) Rink, T. J.; Tsien, R. Y.; Pozzan, T. *J. Cell Biol.* **1982**, *95*, 189−196.

(15) Lopez, J. R.; Alamo, L.; Caputo, C.; Vergara, J.; DiPolo, R. *Biochim. Biophys. Acta* **1984**, *804*, 1−7.

(16) Scarpa, A.; Brinley, F. J. *Fed. Proc.* **1981**, *40*, 2646−2652.

(17) Flatman, P.; Lew, V. L. *Nature* **1977**, *267*, 360−362.

(18) (a) Gupta, R. K.; Gupta, P.; Moore, R. D. *Annu. Rev. Biophys. Bioeng.* **1984**, *13*, 221−246. (b) Wu, S. T.; Pieper, G. M.; Salhany, J. M.; Eliot, R. S. *Biochemistry* **1981**, *20*, 7399−7403. (c) Cohen, S. M. *J. Biol. Chem.* **1983**, *258*, 14294−14308.

(19) (a) Suzuki, Y.; Komatsu, H.; Ikeda, T.; Saito, N.; Araki, S.; Citterio, D.; Hisamoto, H.; Kitamura, Y.; Kubota, T.; Nakagawa, J.; Oka, K.; Suzuki, K. *Anal. Chem.* **2002**, *74*, 1423−1428. (b) Komatsu, H.; Iwasawa, N.; Citterio, D.; Suzuki, Y.; Kubota, T.; Tokuno, K.; Kitamura, Y.; Oka, K.; Suzuki, K. *J. Am. Chem. Soc.* **2004**, *126*, 16353−16360.

(20) Farruggia, G.; Iotti, S.; Prodi, L.; Montalti, M.; Zaccheroni, N.; Savage, P. B.; Trapani, V.; Sale, P.; Wolf, F. I. *J. Am. Chem. Soc.* **2006**, *128*, 344−350.

(21) (a) Rumi, M.; Ehrlich, J. E.; Heikal, A. A.; Perry, J. W.; Barlow, S.; Hu, Z.; McCord-Maughon, D.; Parker, T. C.; Röckel, H.; Thayumanavan, S.; Marder, S. R.; Beljonne, D.; Brédas, J.-L. *J. Am. Chem. Soc.* **2000**, *122*, 9500−9510. (b) Ventelon, L.; Charier, S.; Moreaux, L.; Mertz, J.; Blanchard-Desce, M. *Angew. Chem., Int. Ed.* **2001**, *40*, 2098−2101. (c) Cho, B. R.; Son, K. H.; Lee, S. H.; Song, Y.-S.; Lee, Y.-K.; Jeon, S.-J.; Choi, J. H.; Lee, H.; Cho, M. *J. Am. Chem. Soc.* **2001**, *123*, 10039−10045. (d) Lee, W.-H.; Lee, H.; Kim, J.-A.; Choi, J.-H.; Cho, M.; Jeon, S.-J.; Cho, B. R. *J. Am. Chem. Soc.* **2001**, *123*, 10658−10667. (e) Chung, S.-J.; Rumi, M.; Alain, V.; Barlow, S.; Perry, J. W.; Marder, S. R. *J. Am. Chem. Soc.* **2005**, *127*, 10844−10845. (f) Lee, S. K.; Yang, W. J.; Choi, J. J.; Kim, C. H.; Jeon, S.-J.; Cho, B. R. *Org. Lett.* **2005**, *7*, 323−326. (g) Yang, W. J.; Kim, D. Y.; Jeong, M.-Y.; Kim, H. M.; Lee, Y. K.; Fang, X.; Jeon, S.-J.; Cho, B. R. *Chem.−Eur. J.* **2005**, *11*, 4191−4198.

(22) Kim, H. M.; Yang, W. J.; Kim, C. H.; Park, W.-H.; Jeon, S.-J.; Cho, B. R. *Chem.−Eur. J.* **2005**, *11*, 6386−3691.

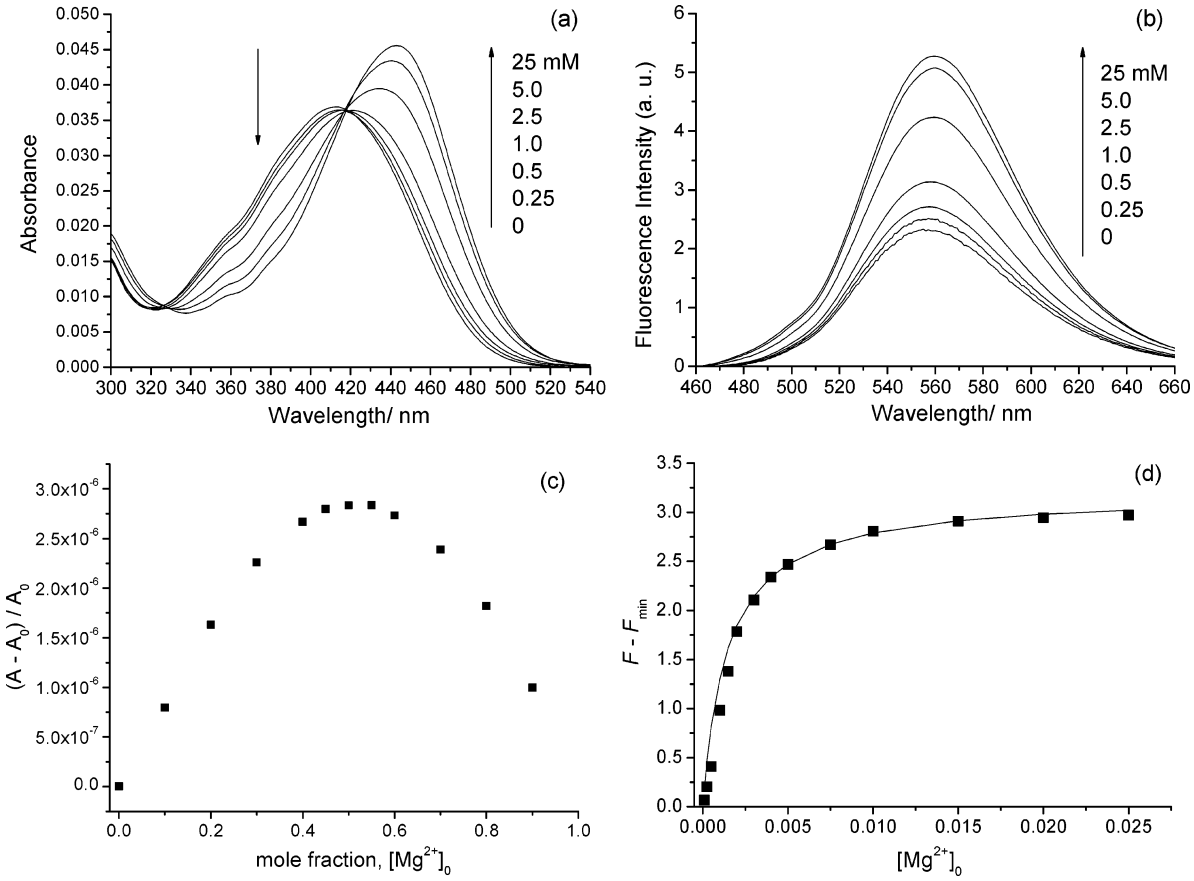

FIGURE 1. One-photon absorption (a) and fluorescence (b) spectra of CMg1 in the presence of various concentrations of Mg^{2+} ions (0−25 mM). Excitation wavelength was 443 nm. (c) Job plot for determination of the stoichiometry of CMg1−Mg^{2+}. The total concentration of CMg1 and Mg^{2+} was maintained to be 2.0×10^{-6} M. (d) One-photon fluorescence titration of CMg1 with various concentrations of Mg^{2+} (0−25 mM). The black squares (■) are the experimental, data and the solid line (−) is the fitted curve by using eq 3. Excitation was provided at 443 nm, and emission intensity was measured at 559 nm. All experiments were conducted in an aqueous micellar solution ([SDS] = 10 mM).

porting Information, Figure S1). The solubility of CMg1 in H_2O is 3.0×10^{-6} M in H_2O, which is sufficient to stain the cells. This indicates that our design strategy is efficient in providing water solubility without attaching a pendent solubilizing group.

The absorption and emission spectra of CMg1−AM showed a gradual bathochromic shift with the solvent polarity in the order 1,4-dioxane < DMF < EtOH < H_2O (Supporting Information, Figure S2). The emission spectra show a larger shift than the absorption spectra (21 vs 80 nm), indicating that the solvent effect is more pronounced in the emitting than in the Franck−Condon state. The large change in λ^{fl}_{max} with the solvent polarity variation indicates the utility of CMg1−AM as the polarity probe.

The UV−vis spectrum changes upon addition of various concentrations of Mg^{2+} gave insight into the binding properties of CMg1 toward Mg^{2+} ions. When Mg^{2+} was added to CMg1 in HEPES buffer (pH 7.0), there was no change in either the absorption or emission spectra. In an aqueous micellar solution containing sodium dodecyl sulfate (SDS, 10 mM), however, the absorption spectra showed a gradual bathochromic shift from 413 to 443 nm. A clean isosbestic point was observed at 418 nm. This result can be attributed to the enhanced acceptor strength of the β-keto acid moiety upon binding with Mg^{2+} (Figure 1a). Similar results were reported for KMGs.[19a] With excitation at 443 nm, a remarkable increase in the fluorescence was observed at increasing Mg^{2+} concentration in SDS solution, although the λ^{fl}_{max} remained nearly constant at 559 nm (Figure 1b). Similar results were observed with Ca^{2+}, except that the changes were smaller (Supporting Information, Figures S3 and S4). Therefore, the dramatic changes in the spectral properties with the solvent can be attributed to the more hydrophobic environment of the SDS which may have facilitated the metal ion binding.[23]

TABLE 1. Effects of SDS and Dioxane Concentration on Binding Properties of CMg1 with Mg^{2+}

[SDS]/mM	K_d/mM	dioxane (vol%)	K_d/mM
0.5	2.3	20	nd[a]
1.0	1.8	40	6.7
5.0	1.6	50	1.1
10	1.3	60	0.34
15	1.3	70	0.05
20	1.4	80	nd[a]

[a] The changes in the fluorescence intensity were too small to accurately measure the K_d.

Supporting evidence for this conclusion has been provided by the effect of the solvent on the binding ability. Table 1 shows that the dissociation constant (K_d) for the complexation of CMg1 with Mg^{2+} decreases gradually with SDS concentration up to 10 mM and then remains constant, indicating that the binding ability is not altered above the critical micellar concentration.

(23) (a) Mallick, A.; Mandal, M. C.; Haldar, B.; Chakrabarty, A.; Das, P.; Chattopadhyay, N. *J. Am. Chem. Soc.* **2006**, *128*, 3126−3127. (b) Zhao, Y.; Zhong, Z. *Org. Lett.* **2006**, *8*, 4715−4717.

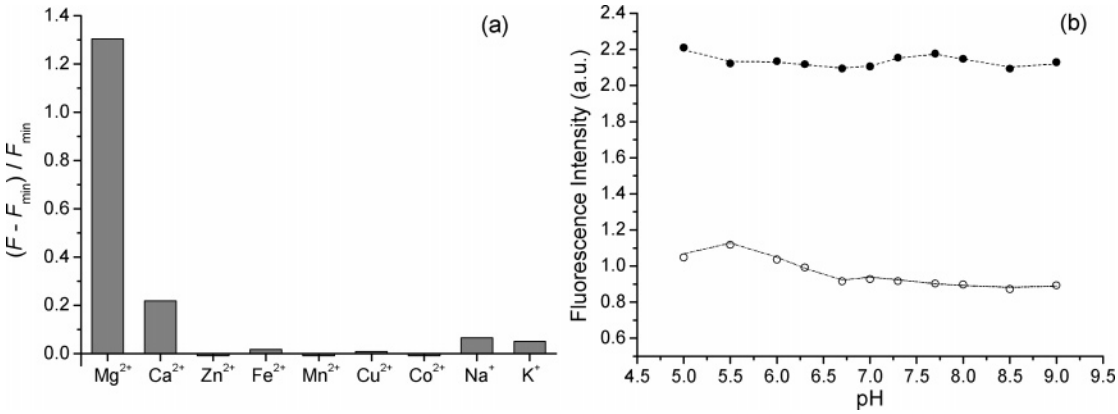

FIGURE 2. (a) The relative fluorescence intensity of CMg1 in the presence of various cations (25 mM for Mg^{2+} and Ca^{2+}; 5 μM for Zn^{2+}, Fe^{2+}, Mn^{2+}, Cu^{2+}, and Co^{2+}; 100 mM for Na^{+} and K^{+}). (b) pH dependency. These data were obtained in an aqueous micellar solution ([SDS] = 10 mM). The emission was monitored at 559 nm with an excitation wavelength of 443 nm.

In an aqueous 1,4-dioxane solution, CMg1 showed negligible binding with Mg^{2+} at 20 vol % 1,4-dioxane(aq), which became more efficient with the 1,4-dioxane concentration, as indicated by the gradual decrease in the K_d value (Table 1 and Supporting Information, Figure S5). This indicates that the binding ability increases with the lipophilicity of the solvent. In 80 vol % 1,4-dioxane(aq), we could not measure the K_d due to the poor solubility of $MgCl_2$. Interestingly, the K_d and λ_{max}^{fl} values measured in SDS solution are very similar to those in 50 vol % 1,4-dioxane(aq), indicating that the polarity of the water−micelle interface, where the probe is expected to reside,[23] is similar to that of the latter. Furthermore, the two-photon titration curves for the complexation between CMg1 and Mg^{2+} in the SDS solution and ionophore-treated Hep3B cell (Figure 3b), as well as the λ_{max}^{fl} values of CMg1 in the SDS solution (Figure 1b) and the two-photon excited fluorescence (TPEF) emitted from the homogeneous domain of the CMg1-labeled Hep3B cell (Figure 4d), were found to be similar. These results seem to indicate that the SDS solution is a good model for the intracellular environment and that CMg1 binds with intracellular free Mg^{2+} in the region with polarity similar to that of the water−micelle interface.

The complexation ratio between the ligand and the metal ion was determined by Job's method. The fluorescence intensity was determined by changing the mole fraction of Mg^{2+} from 0 to 1, while keeping the total concentration of CMg1 and Mg^{2+} at 2.0×10^{-6} M. The plot of $(A - A_0)/A_0$ vs the mole fraction of Mg^{2+} (Figure 1c) exhibits a maximum point at the mole fraction 0.55, indicating a typical ligand−metal complex ratio of 1:1.

The dissociation constants of various probes for Mg^{2+} and Ca^{2+} are summarized in Table 2. The K_d values of CMg1 are 1.3 mM for Mg^{2+} and 3.6 mM for Ca^{2+}, respectively. The $K_{d,Mg}$ value of CMg1 is similar to those of Mag-fura-2, MgG, and KMG-104 but much larger than that of DCHQ. On the other hand, the $K_{d,Mg}/K_{d,Ca}$ ratio of CMg1 is 0.36, which is comparable to those reported for KMGs but much smaller than those for Mag-fura-2 and MgG.[19] Thus, the selectivity of CMg1 for Mg^{2+} vs Ca^{2+} is much higher than those of the commercial Mg^{2+} probes, if not better than KMG-104. Because the intracellular Mg^{2+} concentration (0.1−1.0 mM) is much higher than that of Ca^{2+} in Hep3B cells (40−70 nM),[24] this probe can measure the intracellular free Mg^{2+} ion concentration without interference by Ca^{2+} ions.

TABLE 2. Comparison of the Dissociation Constants of Various Probes for Mg^{2+} and Ca^{2+}

compound	condition	$K_{d,Mg}$[a,b]	$K_{d,Ca}$[a,b]	$K_{d,Mg}/K_{d,Ca}$
CMg1	one photon[c]	1.3 (1.3)	3.6 (0.2)	0.36
	two photon[c]	1.7 (1.3)	3.9 (0.2)	0.44
	two photon[d]	2.5 (0.9)	nd	nd
Mag-fura-2[e]	one photon[f]	1.9 (1.5)	0.025 (0.4)	76
MgG[e]	one photon[f]	1.0 (17)	0.006 (18)	167
KMG-104[g]	one photon[h]	2.1 (7.2)	7.5 (0.6)	0.28
DCHQ[i]	one photon[j]	0.044 (5.1)	−	−

[a] Dissociation constant in mM. [b]The numbers in the parentheses are the fluorescence enhancement factor, $(F - F_0)/F_0$. [c]Measured in an aqueous micellar solution ([SDS] = 10 mM). [d]Measured in ionophore-treated Hep3B cells. [e]Ref 6. [f]Measured in 10 mM Tris, 100 mM KCl, pH 7.05. [g]Ref 19b. [h]Measured in 50 mM Hepes, 130 mM KCl, 20 mM NaCl, pH 7.20. [i]Ref 20. [j]Measured in DPBS buffer.

Figure 2a shows the relative fluorescence intensity of CMg1 in the presence of various cations. CMg1 showed no response toward alkali metal ions (Na^{+}, K^{+}) and transition-metal ions (Zn^{2+}, Fe^{2+}, Mn^{2+}, Cu^{2+}, Co^{2+}), whereas a strong response toward alkaline earth metal ions (Ca^{2+}, Mg^{2+}) was documented. The response is stronger for Mg^{2+} than for Ca^{2+} by approximately 6.5-fold. Therefore, the interference to signal by alkali and transition-metal ions can be excluded. Moreover, the fluorescence intensities of CMg1 and CMg1−Mg^{2+} are nearly constant above pH 6.5; that is, this probe is pH-insensitive in the biologically relevant pH range in SDS solution (Figure 2b).

The TP cross sections (δ_{TPA}) of CMg1, CMg1−Mg^{2+}, MgG−Mg^{2+}, and Mag-fura-2−Mg^{2+} were determined by using the two-photon-induced fluorescence measurement technique as reported.[21a,f] The two-photon excitation spectra (Figure 3a) illustrated that the δ_{max} value of CMg1 is 290 GM at 820 nm. When an excess amount of Mg^{2+} was added to CMg1, $\lambda_{max}^{(2)}$ was shifted to 880 nm and the δ_{max} increased to 382 GM. At 880 nm, the two-photon action cross section ($\Phi\delta_{max}$) of CMg1 increased from 44 to 107 GM upon binding with Mg^{2+}; there was a 2.5-fold enhancement in the two-photon excited fluorescence (TPEF) (Table 3). The change in the TPEF intensity during the binding event is very similar to that observed in the one-photon process (Figure 1b). This allows detecting Mg^{2+}

(24) (a) Bear, C. E.; Li, C. H. *Am. J. Physiol. (London)* **1991**, *261*, C1018−C1024. (b) Fitz, J. G.; Sostman, A. H.; Middleton, J. P. *Am. J. Physiol. (London)* **1994**, *266*, G677−G684. (c) Cho, M. R.; Thatte, H. S.; Silvia, M. T.; Golan, D. E. *FASEB J.* **1999**, *13*, 677−683.

(25) Szmacinski, H.; Lakowicz, J. R. *J. Fluoresc.* **1996**, *6*, 83−95.

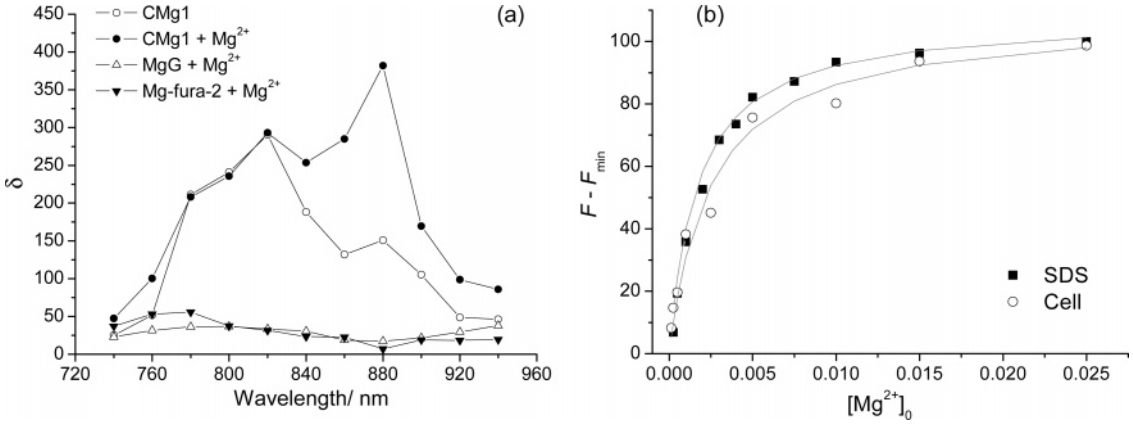

FIGURE 3. (a) Two-photon excitation spectra of CMg1 (○), CMg1−Mg^{2+} (●), Magnesium Green−Mg^{2+} (△), and Mag-fura-2−Mg^{2+} (▼) in aqueous solution (10 mM SDS for CMg1 and CMg1 + Mg^{2+}; 10 mM Tris, 100 mM KCl, pH 7.05 for Mag-fura-2 + Mg^{2+} and MgG + Mg^{2+}). The spectra for the Mg^{2+} ion complexes were obtained in the presence of 35 mM Mg^{2+}. (b) Two-photon fluorescence titration of CMg1 with Mg^{2+} ions in an aqueous micellar solution ([SDS] = 10 mM, ■) and in Hep3B cells (○) in the presence of various concentrations of Mg^{2+} ions (0−25 mM). The excitation wavelength was 880 nm, and emission intensity was integrated in the 560−640 nm region.

TABLE 3. Photophysical Data for Magnesium Ion Probes

compd	solvent	$\lambda_{max}^{(1)}$ [a]	λ_{max}^{fl} [b]	$\lambda_{max}^{(2)}$ [c]	Φ [d]	δ_{max} [e]	$\Phi\delta_{max}$
CMg1	H_2O [f]	413	556	820	0.29	290 (151) [g]	84 (44) [g]
CMg1−Mg^{2+} [h]	H_2O [f]	443	559	880	0.28	382	107
Mag-fura-2−Mg^{2+} [h]	H_2O [i]	330 [j]	491 [j]	780	0.30 [j]	56 (7) [g]	17 (2) [g]
MgG−Mg^{2+} [h]	H_2O [i]	506 [j]	532 [j]	800	0.42 [j]	37 (17) [g]	16 (7) [g]

[a,b] λ_{max} of the one-photon absorption and emission spectra in nm. [c] λ_{max} of the two-photon excitation spectra in nm. [d] Fluorescence quantum yield. [e] The peak two-photon cross section in 10^{-50} cm^4 s/photon (GM). The experimental uncertainty is of the order of 10−15%. [f] Micellar solution containing [SDS] = 10 mM. [g] The numbers in the parentheses are the values at 880 nm. [h] Data were obtained in the presence of 35 mM of Mg^{2+}. [i] 10 mM Tris, 100 mM KCl, pH 7.05. [j] Ref 25.

by TPM. For comparison, the $\Phi\delta$ values for the MgG−Mg^{2+} and Mag-fura-2−Mg^{2+} complexes are <8 GM at 880 nm (Table 3). Hence, CMg1−Mg^{2+} would emit 20-fold stronger TPEF than the latter when excited at this wavelength, a result that underlines the usefulness of this probe for TPM. However, it is difficult to compare the TPEF of CMg1 with those of KMG-104 and DCHQ because the $\Phi\delta$ values of these probes have not been reported.

The two-photon fluorescence titration curves for the complexation of CMg1 with Mg^{2+} and Ca^{2+} in SDS solutions are shown in Figure 3b and Supporting Information Figure S4, respectively. The K_d values for the two-photon processes are 1.7 and 3.9 mM for Mg^{2+} and Ca^{2+}, respectively (Table 2). As expected, the two-photon values are very similar to those measured with the one-photon process.[4b,c]

Photostability was determined in giant unilamellar vesicles (GUVs) formed from a mixture of 1,2-dioleoyl-*sn*-glycero-3-phosphocholine (DOPC) phospholipids and CMg1 (200:1).[22] Because the diffusion rate is expected to be much slower in GUVs than in solution and the DOPC GUV is the most hydrophilic membrane, this result provides a more direct measure of the photostability under imaging conditions than the continuous laser irradiation into the dye solution. The photobleaching rate follows first-order kinetics,[22,26] with a half-life ($t_{1/2}$) of 3070 s (Supporting Information, Figure S6), a stability sufficient for imaging applications. Moreover, the $t_{1/2}$ of CMg1 is 7-fold longer than the 410 s value reported for 1,4-bis[(*E*)-4-(dihexylamino)styryl]benzonitrile under comparable conditions.[22] This observation confirms the usefulness of our design strategy of enclosing the conjugated double bond within a ring to enhance the photostability.

Figure 4a shows the pseudocolored TPEF intensity image of Hep3B cells labeled with 3 μM CMg1−AM collected at 460−640 nm. The image is clear, probably because of the significant $\Phi\delta$ value. It reveals intense spots (red) and bright domains (green). The TPEF spectra of the two regions show λ_{max}^{fl} at 502 nm (blue) and 554 nm (red), respectively (Figure 4d). Both spectra can be fitted to two Gaussian functions with maxima at 499 and 543 nm (sky blue) and at 493 and 554 nm (orange), respectively. Note that the peak positions of the dissected spectra are very similar, suggesting that the probes may be located in two regions with different polarity. To assess their polarity, the lifetime images of the CMg1−AM-labeled Hep3B cells were obtained. The intense spots exhibited the excited-state lifetimes in the range of 2.4−2.9 ns, which were longer than the upper extreme in the lifetime distribution curve centered at 1.6 ns (Figure 5). This result indicates that the probes are located in two different environments, a more polar one that is likely to be cytosol, which gives red emission with a shorter lifetime, and a less polar one that is likely to be membrane associated, which emits blue light with an extended lifetime.

Additional evidence in support of this analysis is provided by the activity of CCCP. Because CCCP prevents ATP−Mg^{2+} production from ADP, inorganic phosphate, and Mg^{2+} by uncoupling oxidative phosphorylation, CCCP-treated cells should have higher levels of free Mg^{2+}.[27] Administration of CCCP to CMg1−AM-labeled Hep3B cells produced an increase in TPEF intensity in the 560−640 nm region immediately after addition of the uncoupler and then a decrease to the baseline level (Figure 4e). In contrast, little change in the TPEF intensity is observed in the range of 460−520 nm. This outcome can only be explained if the former is due to the intracellular CMg1−Mg^{2+} and the latter to the CMg1−AM located in the cell membrane. Moreover, the TPEF emitted from the membrane-associated probes is approximately 16% of the total emission from intracellular CMg1−Mg^{2+} (Figure 4e).

(26) (a) Giloh, H.; Sedat, J. W. *Science* **1982**, *217*, 1252−1255. (b) Benson, D. M.; Bryan, J.; Plant, A. L.; Gotto, A. M., Jr.; Smith, L. C. *J. Cell Biol.* **1985**, *100*, 1309−1323.

(27) Nelson, D. L.; Cox, M.; Lehninger, M. *Principles of Biochemistry*, 4th ed.; W. H. Freeman & Company: New York, 2005; p 707.

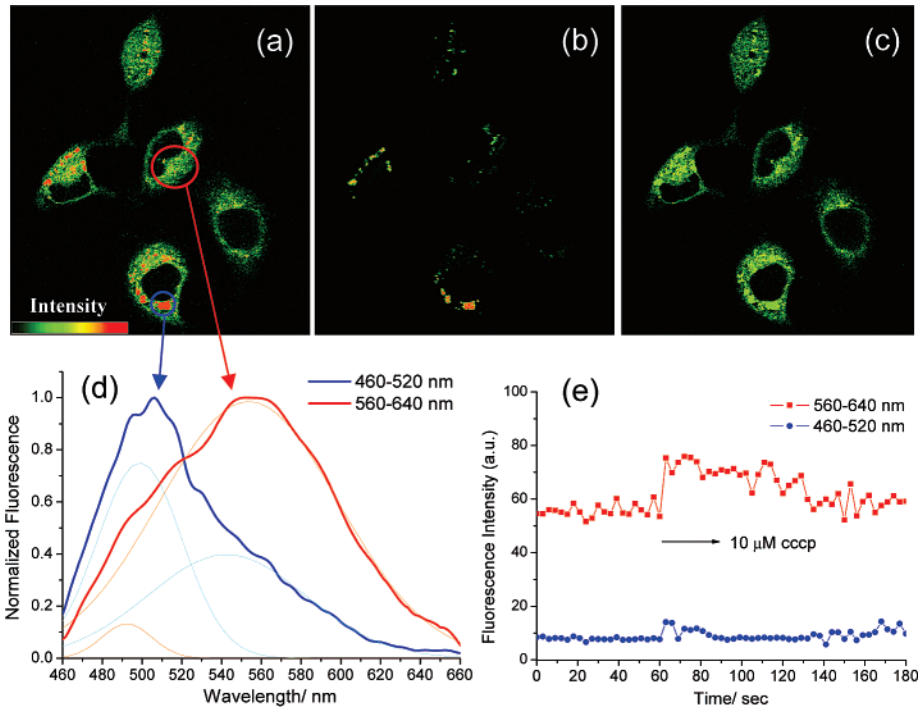

FIGURE 4. Pseudocolored TPM images collected at 460−640 nm (a), 460−520 nm (b), and 560−640 nm (c) of CMg1−AM-labeled (3 μM) Hep3B cells. The excitation wavelength was 880 nm. (d) Two-photon excited fluorescence spectra from the hydrophobic (blue) and hydrophilic (red) domains of CMg1−AM-labeled (3 μM) Hep3B cells. The excitation wavelength was 880 nm. Cells shown are representative images from replicate experiments. (e) TPEF intensity collected at 560−640 nm (red) and 460−540 nm (blue) as a function of time.

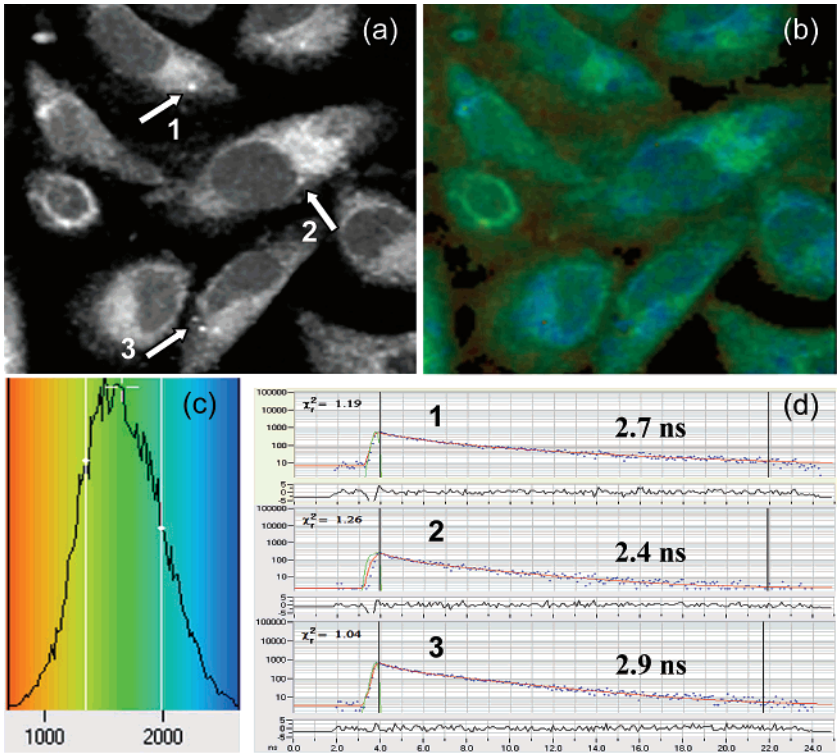

FIGURE 5. (a) One-photon fluorescence intensity image and (b) pseudocolored lifetime image of CMg1−AM-labeled (3 μM) Hep3B cells. The excitation wavelength is 405 nm. (c) Lifetime distribution. The average lifetime is ∼1.6 ns. (d) Single-point analysis of the region indicated by white arrows gives lifetimes in the range 2.4−2.9 ns.

The errors due to the membrane-bound probes can be minimized based on this analysis. As shown in Figure 4d, the shorter wavelength bands in the dissected Gaussian functions decreased to baseline at ∼560 nm. Thus, the TPEF emitted from the membrane-bound probes should be negligible at >560 nm. Therefore, one can selectively detect the TPEF from the intracellular CMg1−Mg^{2+} by using the detection window at 560−640 nm. Consistently, the TPEF image collected at 560−

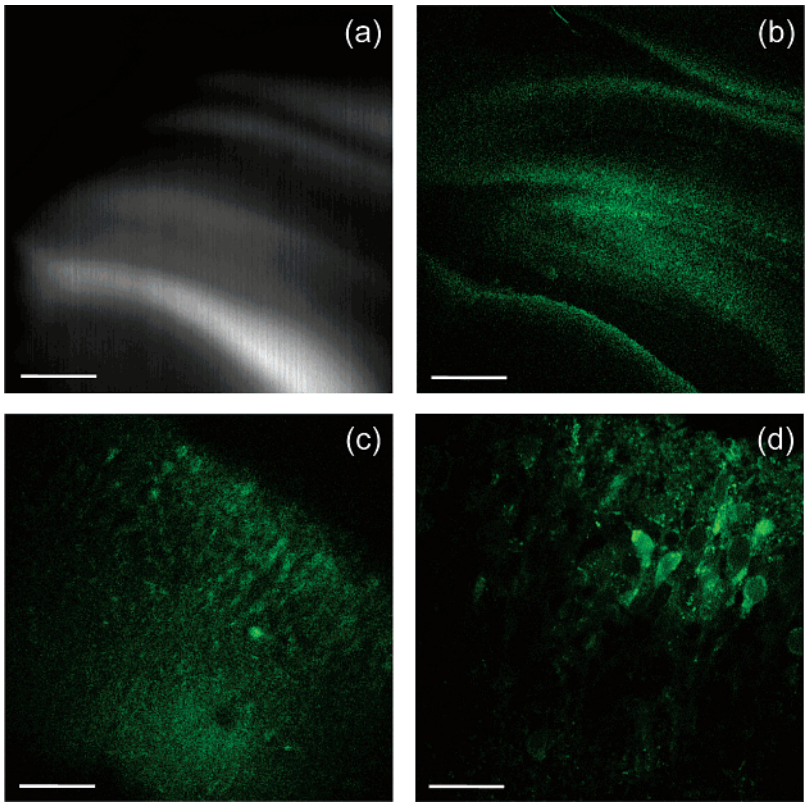

FIGURE 6. Images of a fresh mouse hippocampal slice stained with 10 μM CMg1−AM. (a) A bright-field image (a) and TPEF image (b) show the dentate gyrus and the CA1 region at a depth of 250 μm by magnification at 10×. (c) Magnification at 40× shows the CA1 layer at a depth of 100 μm. (d) Magnification at 100× shows CA1 pyramidal neurons at a depth of 100 μm. Scale bars: 300 (a, b), 120 (c), and 30 (d) μm, respectively. The TPEF images were collected at 560−640 nm upon excitation by 880 nm laser photons.

640 nm is homogeneous without the red spots due to the membrane-bound probes (Figure 4c). In contrast, the red spots can be clearly seen in the images collected using the shorter wavelength window of 460−520 nm (Figure 4b).

To accurately determine the intracellular concentration of Mg^{2+} ions, we have measured the intracellular K_d^i for the two-photon process in the ionophore-treated Hep3B cells by the same procedure as described above (Figure 3b). The K_d^i value is 2.5 mM, 47% larger than that measured in the SDS solution (Table 2). The larger value of K_d^i can be attributed to the possible alteration of the probe properties probably due to the binding to intracellular lipids and proteins. A similar result was reported for fluorescent Mg^{2+} indicator furaptra in rat ventricular myocytes.[28]

The intracellular free Mg^{2+} concentration ($[Mg^{2+}]_i$) was determined by using $[Mg^{2+}]_i = K_d^i[(F - F_{min})/(F_{max} - F)]$.[19,29] The basal $[Mg^{2+}]_i$ in the resting Hep3B cells, as calculated by using the intracellular K_d^i, is 0.56 ± 0.18 mM. The corresponding value, calculated with K_d measured in the SDS solution, is 0.38 ± 0.10 mM. Here again, the value of $[Mg^{2+}]_i$ is larger than the latter. This result underlines the importance of the calibration in the cell interior for the accurate measurement of intracellular Mg^{2+} concentration.

To demonstrate the application of this probe in deep tissue imaging, fresh hippocampal slices from a postnatal 3-day-old mouse were incubated with 10 μM CMg1−AM for 30 min at 37 °C. Figure 6a shows the bright-field image of a part of the mouse hippocampal slice. The TPM images were obtained at 100−300 μm depth by collecting the TPEF over the 560−640 nm range to minimize the contribution by the membrane-bound probes (vide supra). As shown in Figure 6b and Supporting Information Figure S7, the dentate gyrus and the cornu Ammonis 1 (CA1) region are clearly visualized with TPM at 100−300 μm depth. Figures 6c,d display images taken at higher magnification that resolve CA1 pyramidal neurons at 100 μm depth. These experiments clearly show that CMg1 is capable of imaging endogenous stores of free Mg^{2+} at 100−300 μm depth in live tissues using TPM.

In conclusion, we have developed a TP probe (CMg1) that can selectively detect intracellular Mg^{2+} ions in the living Hep3B cells and in live tissues. This probe can be excited by 880 nm laser photons, emits 20-fold stronger TPEF than Mag-fura-2 and MgG in response to Mg^{2+} ions, is easily loaded into the cell and tissue, shows high photostability, and can measure the Mg^{2+} ion concentration without interference by Ca^{2+} ions and membrane-bound probes in living cells. Moreover, the intracellular dissociation constant (K_d^i) for Mg^{2+} determined by the TP process is 2.5 mM, which is suitable for dynamic Mg^{2+} concentration measurement. Finally, CMg1 is capable of imaging endogenous stores of free Mg^{2+} at 100−300 μm depth in live tissues using TPM.

Experimental Section

Synthesis of CMg1. CMg1 was synthesized in two steps starting from **A** (Scheme 1). 6-Dimethylamino-1-hydroxy-3,4-dihydronaph-

(28) Watanabe, M.; Konishi, M. *Pfluegers Arch.* **2001**, *442*, 35−40.
(29) London, R. E. *Annu. Rev. Physiol.* **1991**, *53*, 241−258.

thalene-2-carbaldehyde (**A**) was prepared by the literature procedure.[30] Synthesis of other compounds is described below.

6-Dimethylamino-1-hydroxynaphthalene-2-carbaldehyde (B). A solution of DDQ (2.9 g, 13 mmol) in THF (10.0 mL) was added dropwise to a solution containing **A** (2.8 g, 13 mmol) in THF (30 mL) and stirred for 5 min at room temperature under argon. The solvent was evaporated, and the product was purified on a silica column using CH_2Cl_2 as the eluent. Yield: 1.6 g (57%). IR (KBr, cm^{-1}): 3402 (OH), 1604 (C=O). ^1H NMR (300 MHz, $CDCl_3$) δ 12.85 (s, 1H), 9.77 (s, 1H), 8.27 (d, 1H, $J = 9.0$ Hz), 7.32 (d, 1H, $J = 8.4$ Hz), 7.10 (d, 1H, $J = 8.4$ Hz), 7.08 (dd, 1H, $J = 9.0$ Hz, $J = 2.6$ Hz), 6.76 (d, 1H, $J = 2.6$ Hz), 3.13 (s, 6H). The compound was used immediately after synthesis without further characterization because it decomposed slowly upon standing in the refrigerator.

8-Dimethylamino-2-oxo-2*H*-benzo[*h*]chromene-3-carboxylic Acid Methyl Ester (C). A mixture of **B** (1.0 g, 4.6 mmol), dimethyl malonate (0.66 g, 5.0 mmol), and a catalytic amount of piperidinium acetate in toluene (20 mL) was refluxed in a Dean−Stark trap for 24 h. The mixture was cooled, and the solvent was evaporated. The product was extracted with CH_2Cl_2, washed with brine, and purified by a flash column using hexane/ethyl acetate (3:1) as the eluent. It was further purified by recrystallization from CH_2Cl_2/ethyl acetate. Yield: 0.87 g (64%). Mp 199−200 °C. IR (KBr, cm^{-1}): 1701 (C=O). ^1H NMR (300 MHz, $CDCl_3$) δ 8.64 (s, 1H), 8.44 (d, 1H, $J = 9.5$ Hz), 7.46 (d, 1H, $J = 8.6$ Hz), 7.37 (d, 1H, $J = 8.6$ Hz), 7.21 (dd, 1H, $J = 9.5$ Hz, $J = 2.0$ Hz), 6.91 (d, 1H, $J = 2.0$ Hz), 3.96 (s, 3H), 3.17 (s, 6H). ^{13}C NMR (75 MHz, $CDCl_3$) δ 164.8, 159.9, 157.9, 151.5, 150.7, 139.0, 125.0, 124.9, 123.6, 115.9, 114.1, 112.6, 110.8, 105.7, 52.8, 40.5. Anal. Calcd for $C_{17}H_{15}NO_4$: C, 68.68; H, 5.09; N, 4.71. Found: C, 68.65; H, 4.99; N, 4.61.

8-Dimethylamino-2-oxo-2*H*-benzo[*h*]chromene-3-carboxylic Acid (CMg1). A mixture of **C** (0.5 g, 1.7 mmol) and KOH (0.8 g, 14 mmol) in EtOH/H_2O (20:5 mL) was stirred for 7 h. The resultant solution was diluted with ice−water (20 mL), and concentrated HCl(aq) was added slowly at <5 °C until pH = 3. The resulting precipitate was collected, washed with distilled water, and purified by crystallization from MeOH. Yield 0.4 g (83%). Mp: 285−286 °C. IR (KBr, cm^{-1}): 3435 (OH), 1738 (C=O), 1675 (C=O). ^1H NMR (300 MHz, DMSO-d_6) δ 12.91 (s, 1H), 8.75 (s, 1H), 8.15 (d, 1H, $J = 9.6$ Hz), 7.60 (d, 1H, $J = 8.6$ Hz), 7.52 (d, 1H, $J = 8.6$ Hz), 7.31 (dd, 1H, $J = 9.6$ Hz, $J = 2.4$ Hz), 7.00 (d, 1H, $J = 2.0$ Hz), 3.09 (s, 6H). ^{13}C NMR (75 MHz, DMSO-d_6) δ 165.1, 158.4, 154.4, 151.8, 150.8, 139.0, 126.0, 124.2, 123.7, 116.9, 114.1, 113.5, 111.2, 106.2, 41.5. Anal. Calcd for $C_{16}H_{13}NO_4$: C, 67.84; H, 4.63; N, 4.94. Found: C, 68.85; H, 4.67; N, 4.91.

8-Dimethylamino-2-oxo-2*H*-benzo[*h*]chromene-3-carboxylic Acid Acetoxymethyl Ester (CMg1-AM). A mixture of CMg1 (0.10 g, 0.35 mmol), bromo methylacetate (0.11 g, 0.72 mmol), and Et_3N (0.093 g, 0.72 mmol) in THF (5 mL) was stirred under N_2 for 15 h. The solution was removed in vacuo, and the crude product was purified by column chromatography using hexane/ethyl acetate (2:1) as the eluent. It was further purified by recrystallization from MeOH. Yield 0.11 g (88%). Mp: 200−202 °C. IR (KBr, cm^{-1}): 1763 (C=O), 1625 (C=O). ^1H NMR (300 MHz, $CDCl_3$) δ 8.65 (s, 1H), 8.42 (d, 1H, $J = 9.4$ Hz), 7.44 (d, 1H, $J = 8.6$ Hz), 7.35 (d, 1H, $J = 8.6$ Hz), 7.18 (dd, 1H, $J = 9.4$ Hz, $J = 2.5$ Hz), 6.84 (d, 1H, $J = 2.6$ Hz), 6.00 (s, 2H), 3.17 (s, 6H), 2.15 (s, 3H). ^{13}C NMR (75 MHz, $CDCl_3$) δ 169.9, 168.3, 161.9, 157.3, 155.3, 151.0, 139.1, 125.0, 124.9, 124.6, 123.7, 115.9, 113.6, 110.5, 105.6, 88.7, 46.3, 20.9. Anal. Calcd for $C_{19}H_{17}NO_6$: C, 64.22; H, 4.82; N, 3.94. Found: C, 64.19; H, 4.85; N, 3.91.

Water Solubility. A small amount of CMg1 was dissolved in DMSO to prepare the stock solutions (1.0×10^{-3} M). The solution was diluted to ($6.0 \times 10^{-3} \sim 6.0 \times 10^{-5}$) M and added to a cuvette containing 3.0 mL of H_2O by using a microsyringe. In all cases, the concentration of DMSO in H_2O was maintained to be 0.2%. The plots of fluorescence intensity against the dye concentration were linear at low concentration and showed downward curvature at higher concentration (Supporting Information, Figure S1). The maximum concentration in the linear region was taken as the solubility.

Spectroscopic Measurements. Absorption and fluorescence spectra were recorded on standard spectrometers with a 1 cm standard quartz cell. The fluorescence quantum yield was determined by using Coumarin 307 as the reference by the literature method.[31]

Measurement of a Two-Photon Cross Section. The two-photon cross section (δ) was determined by using the femtosecond (fs) fluorescence measurement technique as described.[21a,f] CMg1, Mag-fura-2, and MgG were dissolved in aqueous solution (10 mM SDS for CMg1; 10 mM Tris, 100 mM KCl, pH 7.05 for Mag-fura-2 and MgG) at concentrations of 3.0×10^{-6} M (CMg1) and 1.0×10^{-5} M (Mag-fura-2 and MgG), and the two-photon induced fluorescence intensity was measured at 740−940 nm by using fluorescein (8.0×10^{-5} M, pH = 11) as the reference, whose two-photon property has been well characterized in the literature.[32] The intensities of the two-photon excited fluorescence (TPEF) spectra of the reference and sample emitted at the same excitation wavelength were determined. The TPA cross section was calculated according to eq 1.

$$\delta = \frac{S_s \Phi_r \phi_r c_r}{S_r \Phi_s \phi_s c_s} \delta_r \qquad (1)$$

Determination of Apparent Dissociation Constants. Aliquots of a stock solution of metal ions ($MgCl_2 \cdot 6H_2O$, $CaCl_2 \cdot 2H_2O$) were added to a cuvette containing a 3.0 mL solution of CMg1 in aqueous solution containing various amounts of sodium dodecyl sulfate (SDS) or aqueous 1,4-dioxane solution. To determine the dissociate constant (K_d), the change in the fluorescence intensity with the metal ion concentration was measured (Figure 1d and Supporting Information, Figure S5).

If a 1:1 metal−ligand complex is formed between CMg1 and Mg^{2+}, one can describe the equilibrium as follows, where L and M represent CMg1 and Mg^{2+}, respectively.

$$L + M \rightleftharpoons LM, \quad K_d = [L][M]/[LM] \qquad (2)$$

The total probe and metal ion concentration are defined as $[L]_0 = [L] + [LM]$ and $[M]_0 = [M] + [LM]$, respectively. With $[L]_0$ and $[M]_0$, the value of K_d is given by:

$$[LM]^2 - ([L]_0 + [M]_0 + K_d)[LM] + [L]_0[M]_0 = 0,$$

$$(F - F_{min}) = \left(\frac{([L]_0 + [M]_0 + K_d) - \sqrt{([L]_0 + [M]_0 + K_d)^2 - 4[L]_0[M]_0}}{2[L]_0}\right)(F_{max} - F_{min}) \qquad (3)$$

where F is the observed fluorescence intensity, F_{min} is the minimum fluorescence intensity, and F_{max} is the maximum fluorescence intensity. The K_d value that best fits the titration curve with eq 3 was calculated by using the Excel program as reported.[33]

To determine K_d for the two-photon process, the TPEF spectra were obtained with a microscope excited by a mode-locked

(30) (a) Bilger, C.; Demerseman, P.; Royer, R. *Eur. J. Med. Chem.* **1987**, *22*, 363−365. (b) Hamilton, R. W. *J. Heterocycl. Chem.* **1976**, *13*, 545−553.

(31) Demas, J. N.; Crosby, G. A. *J. Phys. Chem.* **1971**, *75*, 991−1024.

(32) Xu, C.; Webb, W. W. *J. Opt. Soc. Am. B.* **1996**, *13*, 481−491.

(33) (a) Long, J. R.; Drago, R. S. *J. Chem. Educ.* **1982**, *59*, 1037−1039. (b) Hirose, K. *J. Inclusion Phenom. Macrocyclic Chem.* **2001**, *39*, 193−209.

titanium−sapphire laser source (90 MHz, 200 fs) set at a wavelength of 880 nm and an output power of 1230 mW, which corresponds to approximately 10 mW average power in the focal plane. The TPEF titration curve was obtained and fitted to eq 3.

Photostability. Photostability was determined with a microscope excited by a mode-locked titanium−sapphire laser source (90 MHz, 200 fs) set at a wavelength of 880 nm and an output power of 1230 mW, which corresponds to approximately 14 mW average power in the focal plane. Giant unilamellar vesicles (GUVs) were formed from a mixture of 1,2-dioleoyl-*sn*-glycero-3-phosphocholine (DOPC) phospholipids and CMg1 (200:1).[22] They emit intense TPEF throughout the equatorial sections of GUVs when excited by the polarized light, indicating no photoselection effect and that the dye is easily loaded and randomly oriented in the GUVs (Supporting Information, Figure S6).[34] To determine the decay rate of the TPEF intensity of the dyes in GUVs, the digitized intensity (8 bit) from the GUV images was recorded with 1.63 s intervals for the duration of 1 h using the *xyt* mode (λ = 880 nm, ∼200 fs). The TPEF of the dye-labeled GUVs (∼40 μm) was collected using a ×20 objective lens (NA = 0.50 DRY). The plot of $\ln(I - I_\infty)/(I_o - I_\infty)$ vs irradiation time for the GUVs labeled with CMg1 is linear (Supporting Information, Figure S6). The slope of this plot is the first-order decay constant. The half-life ($t_{1/2}$) was calculated by using the relationship, $t_{1/2} = 0.693/k$. The $t_{1/2}$ value of CMg1 is 3070 s.

Cell Culture. Hep3B cells were cultured in Dulbecco's modified Eagle's medium (DMEM) supplemented with penicillin/streptomycin and 10% fetal bovine serum (FBS) in a CO_2 incubator at 37 °C. Hep3B cells were washed three times with serum-free media and then incubated with 3 μM CMg1−AM in serum-free media for 30 min at 37 °C. The cells were washed three times with serum-free media and then imaged after further incubation in serum-free media for 15 min.

Two-Photon Fluorescence Microscopy. Two-photon fluorescence microscopy images of CMg1−AM-labeled Hep3B cells were obtained with spectral confocal and multiphoton microscopes with a ×100 oil objective and numerical aperture (NA) = 1.30. The two-photon fluorescence microscopy images were obtained by exciting the probes with a mode-locked titanium−sapphire laser source (90 MHz, 200 fs) set at a wavelength of 880 nm. To obtain images at 460∼640, 460∼520, and 560∼640 nm ranges, internal PMTs were used to collect the signals in 8 bit unsigned 512 × 512 pixels at 400 Hz scan speed.

Fluorescence Lifetime Imaging Microscopy (FLIM). Hep3B cells were grown on a coverslip in 10% FBS containing DMEM. Cells were washed briefly in PBS and incubated with 3 μM CMg1−AM for 30 min at 37 °C. The cells were washed with PBS three times, fixed with formaldehyde (3.7% in PBS) for 10 min, washed with PBS three times, and then mounted with mounting solution. The fluorescence decays were resolved by time-correlated single-photon counting (TCSPC) using an acquisition board synchronized with a confocal microscope.

Calibration of CMg1 in Hep3B Cells. Intracellular calibration of resting $[Mg^{2+}]_i$ was performed by using a modified literature method.[28,35] To equilibrate extra and intracellular $[Mg^{2+}]$, cells were incubated in various $MgCl_2$ concentrations (0, 0.25, 0.5, 1.0, 2.5, 5, 10, 15, and 25 mM) containing PBS solution with 10 μM calcimycin for 30 min and washed with the same PBS three times. Cells were stained with 3 μM CMg1−AM for 30 min at 37 °C and washed an additional three times with PBS. Cells were fixed with 3.7% formaldehyde in PBS for 10 min, washed with PBS, and then mounted with mounting solution. The two-photon fluorescence intensity of the resulting CMg1−AM-labeled Hep3B cells was measured at the 560∼640 nm range by the same procedure as described above (value from each 500 cells).

$[Mg^{2+}]_i$ at rest was calculated following a conventional formula for single excitation dyes: $[Mg^{2+}]_i = K_d\ [(F - F_{min})/(F_{max} - F)]$,[19,29] where F is the observed TPF intensity. F_{min} was determined with 10 μM calcimycin in the presence of 2 mM EDTA to deplete endogenous Mg^{2+}. F_{max} was estimated with 10 μM calcimycin in the presence of 30 mM $MgCl_2$.[20,35a]

Preparation and Staining of Acute Mouse Hippocampal Slice. Slices were prepared from the hippocampi of 3-day-old mice (C57BL/6). Coronal slices were cut into 400-μm-thick slices using a vibrating-blade microtom in artificial cerebrospinal fluid (ACSF; 138.6 mM NaCl, 3.5 mM KCl, 21 mM $NaHCO_3$, 0.6 mM NaH_2PO_4, 9.9 mM D-glucose, 1 mM $CaCl_2$, and 3 mM $MgCl_2$). Slices were incubated with 10 μM CMg1−AM in ACSF bubbled with 95% O_2 and 5% CO_2 for 30 min at 37 °C. Slices were then washed three times with ACSF and transferred to glass-bottomed dishes (MatTek) and observed in a spectral confocal multiphoton microscope.

Acknowledgment. This work is supported by KRF-2004-201-C00067 and CRM-KOSEF. J. H. Hong and K. J. Lee were supported by Creative Research Initiatives of the Korean Ministry of Science and Technology. We thank Dr. Ji Ho Kim, Institut Pasteur Korea, for FLIM imaging.

Supporting Information Available: Additional figures. This material is available free of charge via the Internet at http://pubs.acs.org.

JO062341M

(34) (a) Bagatolli, L. A.; Gratton, E. *Biophys. J.* **1999**, *77*, 2090−2101. (b) Bagatolli, L. A.; Gratton, E. *Biophys. J.* **2000**, *78*, 290−305.

(35) (a) Reynolds, I. J. *Current Protocols in Neuroscience*; Wiley: New York, 1998. (b) Petr, M. J.; Wurster, R. D. *Cell Calcium* **1997**, *21*, 233−240. (c) Sharikabad, M. N.; Østbye, K. M.; Brørs, O. *Am. J. Physiol.: Heart Circ. Physiol.* **2001**, *281*, H2113−H2123.